

Microstructure and multifunctional properties of liquid + polymer bicomponent structural electrolytes: Epoxy gels and porous monoliths

Edwin B. Gienger, Phuong-Anh T. Nguyen, Wai Chin, Kristopher D. Behler, James F. Snyder, Eric D. Wetzel

U.S. Army Research Laboratory, Materials and Manufacturing Science Division, Aberdeen Proving Ground, Maryland 21005

Correspondence to: E. Wetzel (E-mail: eric.d.wetzel2.civ@mail.mil)

ABSTRACT: Multifunctional structural batteries and supercapacitors have the potential to improve performance and efficiency in advanced lightweight systems. A critical requirement is a structural electrolyte with superior multifunctional performance. We present here structural electrolytes prepared by the integration of liquid electrolytes with structural epoxy networks. Two distinct approaches were investigated: direct blending of an epoxy resin with a poly(ethylene-glycol) (PEG)- or propylene carbonate (PC)-based liquid electrolyte followed by in-situ cure of the resin; and formation of a porous neat epoxy sample followed by backfill with a PC-based electrolyte. The results show that *in situ* cure of the electrolytes within the epoxy network does not lead to good multifunctional performance due to a combination of plasticization of the structural network and limited percolation of the liquid network. In contrast, addition of a liquid electrolyte to a porous monolith results in both good stiffness and high ionic conductivity that approach multifunctional goals. © 2015 Wiley Periodicals, Inc. *J. Appl. Polym. Sci.* **2015**, *132*, 42681.

KEYWORDS: composites; gels; properties and characterization; structure–property relations

Received 11 March 2015; accepted 30 June 2015

DOI: 10.1002/app.42681

INTRODUCTION

Multifunctional structures have the potential to improve performance and efficiency in advanced lightweight systems by bearing mechanical loads while simultaneously providing an additional, distinct capability.^{1–5} Utilization of multifunctional structures can enable significant weight reduction and improve form factors in platforms that range from electric vehicles to mobile phones to satellites. Composite materials are particularly well-suited for multifunctional structures, as the integration of multiple constituents into a single structure provides a wide range of options for selecting materials and stacking sequences that can be exploited for nonstructural functionalities.³

Fiber–matrix composites are of particular interest for developing structural batteries, supercapacitors and capacitors.^{1,3,6–12} Carbon fibers have been shown to be effective as electrodes, where charges are stored.^{13–15} For structural capacitors, polymers, and insulating reinforcement have been shown to act as effective dielectric materials for energy storage.^{8,9} In contrast, electrochemical devices, such as structural batteries and supercapacitors require a matrix/electrolyte that is capable of long-range mass transfer of ionic charges. There is significant competition between the need for rigidity, which is desirable for structural stiffness, and the need for mobility, which is desirable for ion conductivity.

There has been substantial interest in mechanically robust electrolytes for several decades owing to their promise for enabling solid state batteries.^{16,17} Much of this work has been focused on self-supporting flexible membranes. Detailed analysis of multifunctionality in higher modulus (1 MPa–1 GPa) homogenous polymer electrolytes revealed a tradeoff in mechanical and electrochemical properties, with no single material providing both high mechanical properties and high ionic conductivity.¹⁸ Investigation of copolymer systems indicated that the mechanical–electrochemical tradeoff could be manipulated by attributing each of the competing functions, mechanical rigidity and ion conductivity, to distinct monomeric segments within the copolymer.¹⁹ Multifunctionality in these systems was found to be highest when copolymers were formed from monomer pairs consisting of a high stiffness polymer and a high conductivity polymer. However, although these copolymer electrolyte properties were superior to the prior homopolymer results, the multifunctional performance of these systems did not reach desired performance goals. It was hypothesized that multifunctionality could be improved by a more distinct segregation of the functional subcomponents of the polymer, and by exercising additional control of the details of the resulting microstructure. These findings are consistent with theoretical predictions of optimal three-dimensional structures for multi-mode transport.²⁰

Based on these conclusions, structural electrolytes comprising a liquid ion carrier and high modulus framework have been formulated, with vinyl ester and epoxy networks cured in the presence of liquid electrolytes²¹ and ionic liquids^{22,23} showing significant improvements in multifunctional performance. However, this *in situ* polymerization approach has a number of limitations. The presence of the liquid electrolyte can plasticize the structural polymer, reducing overall mechanical stiffness. Ionic liquids can also interfere with the curing processes of the structural phase, potentially limiting the available range of microstructures and use in typical manufacturing techniques for composites. Phase separation is common in these systems, but the resulting microstructure is highly dependent on the properties of the liquid electrolyte phase, for which there may be limited options for tailorability. Finally, many structural resins require elevated temperature cure at conditions under which the electrolyte may volatilize.

We present here a new approach towards developing structural electrolytes in which formation of the structure and introduction of the electrolyte are done in sequence to better optimize each material. We use polyethylene glycol (PEG) as a porogen to generate an epoxy foam,^{24–26} then remove the PEG and backfill the voids with a more conductive propylene carbonate (PC) based electrolyte. Compared with previous approaches, this methodology allows for the microstructure to be tailored independently from liquid electrolyte selection, which greatly widens the range of materials, processing conditions, and microstructures that can be tailored to achieve optimal final properties. We compare in detail the microstructure and properties of this system relative to the same epoxy cured in the presence of a PEG-based electrolyte and a PC-based electrolyte.

EXPERIMENTAL

Materials and Processing

Three material systems were investigated for this study using the basic construct of a liquid electrolyte integrated with a polymer network comprising EPON 828 resin (a diglycidyl ether of bisphenol A, Momentive) and Amicure PACM (4,4'-methylene-biscyclohexanamine) curing agent (Air Products). Systems A and B were prepared by curing the resin in the presence of the electrolyte. System C was prepared by curing the resin in the presence of a soluble porogen that phase separates during cure. After cure, the porogen was removed and replaced by liquid electrolyte.

System A utilized a liquid electrolyte comprising 1.0M lithium bis(trifluoromethane) sulfonamide (LiTFSI) (Sigma Aldrich) in propylene carbonate (PC) (Sigma Aldrich). The electrolyte was prepared in a glovebox under dry, inert atmosphere and stored over molecular sieves until use. Quantities of EPON 828 and PACM were mixed at a 100 : 28 mass ratio. In a glovebox, the electrolyte was then added to achieve the desired composition, which was varied from 0 to 90 wt % electrolyte. Equivalent volume fractions, more meaningful than weight fractions to discussions of properties, were calculated from component densities and used throughout the analyses. The components were cured in silicone molds at room temperature for 48 hours followed by 80°C for 2 h all under dry atmosphere.

System B utilized a liquid electrolyte comprising 1.0M LiTFSI in polyethylene glycol (PEG) (MW 200; Sigma Aldrich). The components were prepared and processed using the same procedures as System A.

System C utilized a surfactant comprising a triblock copolymer of PEG and polypropylene glycol (PPG), PEG-PPG-PEG (MW 1100; Sigma Aldrich), and PEG 200 as porogen in a process modified from that reported elsewhere.²⁶ System C contained 27.5% EPON 828, 7.5% PACM, 60% PEG 200, and 5% surfactant by weight. PEG and surfactant were combined and homogenized for 5 min using a PowerGen Model 1000 S1 (Fisher Scientific) homogenizer with a 7 × 65 mm generator tip, operating at 25,000 rpm. EPON 828 was then added to the mixture, which was further homogenized for 10 min. These three components are miscible and homogenize to a transparent liquid. PACM curing agent was then added to the mixture, which was homogenized for another 15 min. A quantity of 100 g of the mixture was then poured into vertically oriented steel molds with interior volume measuring 125 × 125 × 12.5 mm that had been preheated to 160°C. The samples were held at 160°C for 2 h in an oven, then the oven was turned off, and allowed to slowly cool to room temperature with the door closed. The resulting block was cut into the desired geometries for testing using a water jet. To extract the PEG, cut samples were sonicated in a 50 : 50 water: methanol mixture for 2 h and then soaked in water for 16 h. The samples were dried under vacuum for 16 h at room temperature followed by 4 h under vacuum at 120°C. Half of the samples were backfilled for 16 h with an electrolyte comprising 1.0M LiTFSI in PC. The difference in masses before and after uptake of the electrolyte was used to determine an accessible void volume of about 50%.

Characterization

Dynamic Mechanical Analysis (DMA). DMA was performed on 20 × 12 × 2 mm prismatic bars using a TA instruments DMA Q800. Experiments were performed in the dual cantilever configuration from -150 to 200°C at a heating rate of 2°C/min, with a frequency of 1 Hz and an amplitude of 4 μm. The glass transition temperature (T_g) for each sample was determined from the maximum of the tan δ peak. The modulus at room temperature (E') was estimated from the storage modulus value at 20°C. Samples from System B containing greater than 65 vol % PEG 200 were not able to be tested due to low mechanical robustness.

Thermogravimetric Analysis (TGA). To determine the presence of residual PEG, TGA was performed on 10 mg pellets of System C taken from the interior of the cured block after it had been dried. Samples were tested under nitrogen in a TA instruments TGA Q5000 at a rate of 10°C/min.

Compression Testing. Compressive elastic modulus was measured based on ASTM Standard D695—Compressive Properties of Rigid Plastics.²⁷ Cylindrical disc samples with a thickness of 3–4 mm and a diameter of 12 mm were compressed in an MTS Synergie series electromechanical load frame with a 5 kN load cell. Before samples were tested, the platen heads were compressed against each other to get a measure of compliance in the system that was later taken into account in the data analysis.

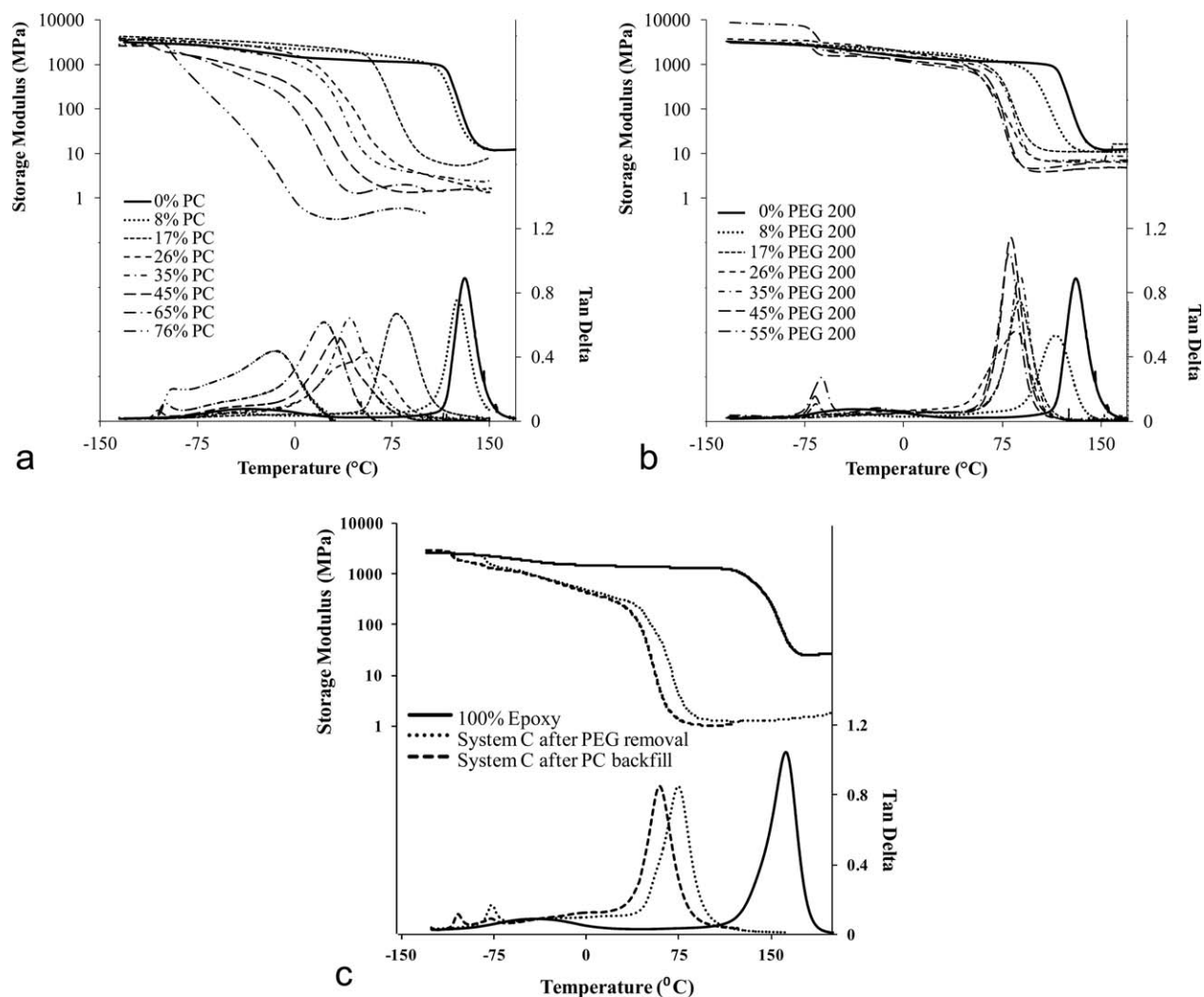


Figure 1. (a) DMA results for System A. (b) DMA results for System B. (c) DMA results for System C.

Samples were compressed at 2 mm/min until the load reached 3 kN, the samples failed, or the load plateaued and began to decrease. The reported compression modulus values were calculated by taking the slope of the linear section of the stress-strain curve after initial loading and before plastic deformation, typically between 2 and 4% strain. Results from at least three samples for each formulation were averaged to achieve the reported values. Over all compression data sets, the average coefficient of variation for a given data set was about 30%.

Electrochemical Impedance Spectroscopy (EIS). Electrochemical impedance spectroscopy was performed using the Autolab series PGSTAT30 with a two electrode setup. The frequency range of interest was 10 to 10^6 Hz at room temperature. Disc-shaped samples, identical in geometry to the compression samples, were used for testing. Samples were lightly sanded on the surface with 200 grit sandpaper to remove any epoxy skin and to expose the porosity. Results from at least three samples for each formulation were averaged to achieve the reported values. Over all conductivity data sets, the average coefficient of variation for a given data set was about 30%. Reliable conductivity measurements were not achieved using our apparatus for samples con-

taining greater than 85 vol % PEG and 75 vol % PC due to poor mechanical integrity and low stiffness.

RESULTS

Table I summarizes the characterization data measured for the sample sets containing epoxy and liquid electrolyte materials. Figure 1(a) shows the DMA results for System A. The T_g drops substantially with increasing electrolyte content. For the samples containing at least 26 vol % PC there is also a substantial decrease in the glassy modulus and broadening of the temperature range of the transition, clearly evident in the increasing width of the primary $\tan \delta$ peak. The low onset temperature of the glass transition in these samples contributes to a rapid reduction in E' at 20°C with increasing concentration of PC. At very high concentrations (≥ 76 vol %) of PC, the System A polymers are in the rubbery viscoelastic regime at 20°C.

Figure 1(b) shows the DMA results for System B. The T_g drops considerably as electrolyte content increases to 26 vol %, but then remains relatively constant with increasing electrolyte content. The small reduction in T_g for the polymers with >26 vol % electrolyte is coupled with similarly small changes in the

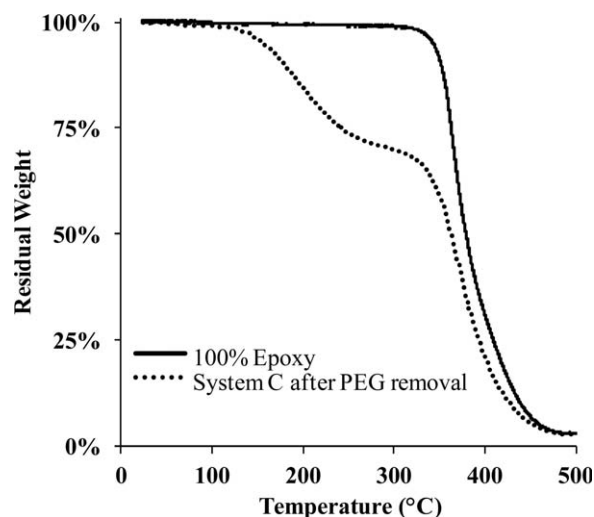


Figure 2. TGA results for System C.

transition width and glassy and rubbery moduli. These minor changes suggest much less of a plasticizing effect as larger quantities of PEG are used.

Figure 1(c) shows the DMA results for System C after removal of the PEG porogen. System C, polymerized with 65 vol % PEG, shows a T_g and room temperature glassy modulus that are slightly lower than that of System B at 55 vol % PEG.

Systems A and B in Figure 1 each exhibit a low temperature transition ($T < -50^\circ\text{C}$) that is attributed to free liquid electrolyte not directly associating with the polymer network. These peaks are not apparent in neat epoxy and increase in size with increasing quantity of liquid. Both peaks are evident in System C in Figure 1(c), suggesting that some PEG remains in the sample even after it has been thoroughly washed and backfilled with PC electrolyte. This hypothesis is further validated by TGA curves for neat epoxy and System C after PEG has been removed via washing, shown in Figure 2. The initial loss of about 30% of the mass of System C likely corresponds to PEG 200 that may have been trapped by, or strongly interacted with, the epoxy network.

Figure 3 shows representative stress–strain curves for compression of each system using samples produced using similar volume fractions of liquid. The neat epoxy sample is considerably stiffer than the polymers cured in the presence of liquids. Systems B and C show comparable stiffnesses, while System A shows the lowest stiffness. The nearly identical modulus value and curve shape for filled and unfilled System C samples indicate minimal impact of the PC backfill on the mechanical properties of the epoxy network. Considering all of the compression data shown in Table I, the trends in compressive modulus versus composition are very similar to those of storage modulus, although the specific values can differ substantially due to differences in the two test methods.

Figure 4 presents SEM micrographs for samples from System A with 26 and 65 vol % PC. The images are similar and devoid of features that would indicate microstructures or phase separation. Figure 5 presents micrographs for samples from System B

with 26, 45, and 65 vol % PEG 200; and System C that was generated using 65 vol % PEG200 as a porogen. The images exhibit noticeable differences in microstructure as the composition varies. The System B sample with 26 vol % PEG [Figure 5(a)] appears as a single-phase material, similar to System A. The System B sample with 45 vol % PEG [Figure 5(b)] and the System C sample generated with 65 vol % PEG [Figure 5(c)] appear as similarly porous materials. It should be noted that the PEG has already been removed from the sample in Figure 5(c), and any free liquid PEG in System B would likely evaporate during the high vacuum conditions required for SEM imaging. The System B sample with 65 vol % PEG [Figure 5(d)] exhibits a porous epoxy structure that appears as interconnected beads.

DISCUSSION

Systems A and B: Morphology and Thermomechanical Properties

The DMA data for Systems A and B suggests a transition from rigid, high T_g systems to compliant, low T_g systems as the base epoxy is cured in the presence of increasing percentages of liquid electrolyte. Figure 6 compares the relationship between T_g and fractional composition of liquid electrolyte with that predicted by the Fox equation:²⁸

$$\frac{1}{T_{g,\text{composite}}} = \frac{w_{\text{epoxy}}}{T_{g,\text{epoxy}}} + \frac{w_{\text{electrolyte}}}{T_{g,\text{electrolyte}}} \quad (1)$$

We used here for $T_{g,\text{electrolyte}}$ the standard T_m values for each base solvent. The Fox equation is reliable for accurately predicting T_g in highly miscible blends of polymers or diluents in polymer. System A [Figure 1(a)] demonstrates some deviation at higher electrolyte content suggesting reasonable solubility through ~40 wt % (35 vol %) electrolyte and imperfect mixing at higher concentrations. System B [Figure 1(b)] holds to the Fox equation only up until ~30 wt % (26 vol %) liquid

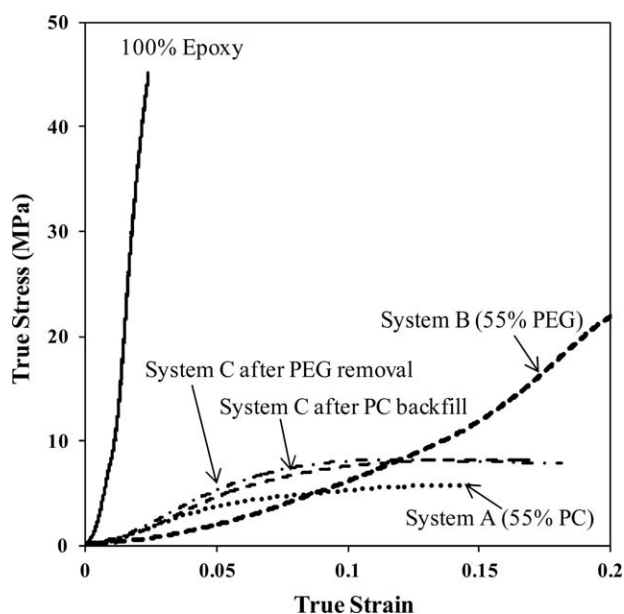


Figure 3. Compression stress–strain data for neat epoxy, System A at 55 vol % PC, System B at 55 vol % PEG, System C after PEG removal, and System C after addition of PC.

Table I. Summary of the Characterization Data

Electrolyte content (vol %)	System A			System B			System C					
	T_g (°C)	E' (MPa)	E_c (MPa)	σ (S/cm)	T_g (°C)	E' (MPa)	E_c (MPa)	σ (S/cm)	T_g (°C)	E' (MPa)	E_c (MPa)	σ (S/cm)
0	140	1300	2000	0	140	1300	2000	0				
8	126	2100	1100	0	116	1800	1200	0				
17	77	2300	850	0	88	1700	1300	0				
26	55	550	150	0	86	1500	930	0				
35	42	330	77	0	88	1300	650	0				
45	37	88	63	2.8×10^{-6}	81	1100	440	0				
55	32	42	66	8.8×10^{-7}	81	940	160	6.0×10^{-6}				
65	23	5.2	17	4.1×10^{-4}	-	-	5	8.8×10^{-5}	74	320	120	1.5×10^{-3}
76	-13	0.35	2	6.6×10^{-4}	-	-	-	-	-	-	-	-
88	-	-	-	-	-	-	-	-	-	-	-	-
100	-49 (T_m)	-	-	5.1×10^{-3}	-65 (T_m)	-	-	4×10^{-4}	-49 (T_m)	-	-	5.1×10^{-3}

T_g = glass transition temperature, E' = DMA storage modulus at 20°C, E_c = compressive modulus at room temperature. Conductivity (σ) data for 100% electrolyte are taken from Ref. (30) for PC (Systems A and C) and estimated from Ref. (31) for PEG 200 (System B). The melting temperatures are standard values for the pure solvents and are expected to depress slightly with incorporation of lithium salt. Dashes indicate samples that were fabricated but were not sufficiently robust to characterize.

electrolyte, after which it deviates more substantially from the predicted trend suggesting little interaction of the additional PEG with the epoxy network. These trends in T_g suggest that System A is more continuously plasticized by PC over the full range of electrolyte content, while System B is plasticized up to around 26 vol % PEG, after which further introduction of electrolyte is only minimally plasticized into the host polymer network.

This interpretation is supported by the microscopy. System A appears to contain minimal phase separation such that the epoxy network is continuously plasticized over most electrolyte concentrations. For System B, the 26% PEG sample appears homogenous, while above 45% PEG the porous epoxy microstructure suggests excess PEG has phase separated, with higher PEG content leading to a connected-sphere morphology typically of liquid-rich phase separated systems.^{24–26} These observations indicate that the PEG has limited miscibility with the epoxy monomer or resulting network.

The differences in microstructure and electrolyte-epoxy interaction for Systems A and B are also likely responsible for the large differences in their compressive moduli at higher electrolyte content. System A exhibits a stronger decline in compressive stiffness at low electrolyte concentrations, while System B appears to better resist degradation in its structural properties from 17 to 55% electrolyte. This trend further supports the hypothesis that the properties of the epoxy networks in System A are dominated by increasing homogenous plasticization, while in System B they are only compromised by limited plasticization (~26% electrolyte) with excess electrolyte acting instead as porogens to reduce network volume fraction. The very low compressive moduli and lack of sufficient structural coherence to achieve good DMA measurements in System B at 65–76% PEG reflect the change in network structure from that of porous monolith [Figure 5(b)] to weakly interconnected spheres [Figure 5(d)].

Systems A and B: Ionic Conductivity

For System A, conductivity is very low up to 55% electrolyte content. This result indicates that the epoxy network itself, even when plasticized with moderate levels of PC, does not substantially support ion transport. In contrast, previous results have shown that structural networks derived from PEG-based vinyl esters do demonstrate measureable and steadily increasing ion conductivity as 0–35% liquid electrolyte is included.²¹ A significant increase in conductivity is observed for System A at 65% electrolyte. The DMA data for System A also shows the emergence and growth of a low temperature $\tan \delta$ peak in Figure 2(a) at electrolyte content of 55% and above. The secondary transition is attributed to a PC-rich phase.²⁹ These results, taken together, could suggest that PC electrolyte begins to phase separate and percolate at these higher loadings. However, the micrographs in Figure 5(d) show little evidence of bulk phase separation or porosity at 65% electrolyte and the conductivities of the samples remain one order of magnitude lower than neat PC. Therefore, the PC network may be very fine in scale and minimally percolated.

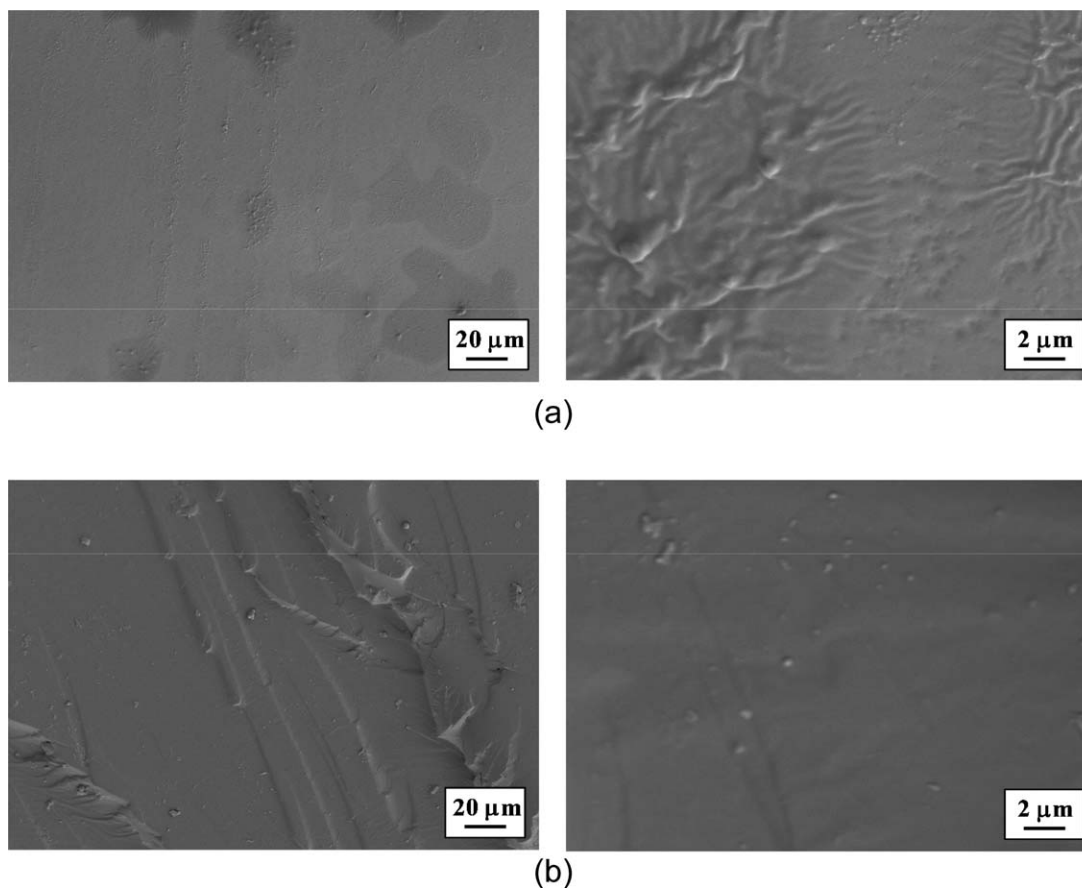


Figure 4. Micrographs of (a) System A, 26 vol % PC and (b) System A, 65 vol % PC.

For System B, conductivity is negligible through electrolyte content of 45%, although phase separation is evident at 45% electrolyte [Figure 5(b)]. These results indicate that the PEG-plasticized epoxy is not inherently conductive, and that the phase separated liquid PEG domains at 45% are not fully percolated. At 55 and 65% electrolyte content conductivity increases, indicating a percolated phase-separated structure consistent with the micrograph in Figure 5(d).

System C

Comparing System C fabricated with 65% PEG to System B with 55–65% PEG electrolyte, the T_g and mechanical properties of the two systems are comparable. However, the conductivity of System C after porogen removal and replacement with PC electrolyte is considerably better than that of System B, by one or two orders of magnitude. The primary contributor to this difference may be higher conductivity of the PC electrolyte compared to PEG electrolyte. Further improvements may be achieved by targeting conductivity in this electrolyte phase through alternative solvents, alternative ions, alternative concentration of ions and at higher operating temperature. A second contributor to the improvement noted in System C could be the microstructure of the System C monolith compared to System B, although it is difficult to make quantitative judgments on percolation and transport by visually comparing Figures 5(b–d).

Multifunctional Performance

Figure 7 plots ionic conductivity as a function of compressive stiffness for the materials evaluated in this study. As noted in the Introduction, a reasonable goal for a structural electrolyte is to achieve each of mechanical stiffness and ion conductivity within one order of magnitude of conventional materials. Considering our base epoxy (2000 MPa compressive stiffness) and PC liquid electrolyte (5.1 mS/cm conductivity), a good structural electrolyte should achieve at least 200 MPa compressive stiffness and 0.5 mS/cm conductivity. These boundaries are marked in Figure 7. The idealized rule of mixtures tradeoff in conventional performance for these materials is also indicated.

System A, which uses high performance materials for both structure and electrolyte, provides a good range of tailorable properties but an unacceptable tradeoff between conductivity and modulus. This trend indicates that binary plasticized structure–electrolyte systems, without distinct phase-separated phases, may be unsuitable for multifunctional electrolytes. The close interaction of the structural and electrolyte polymers appears to significantly compromise their individual functions.

Systematic multifunctional performance cannot be determined in System B due to the experimental difficulties associated with measurements in the 76–88% electrolyte systems, but neither are the results inconsistent with generally expected trends. In addition, the dramatic changes in structure at 55–65% electrolyte lead to a drastic reduction in mechanical response. These

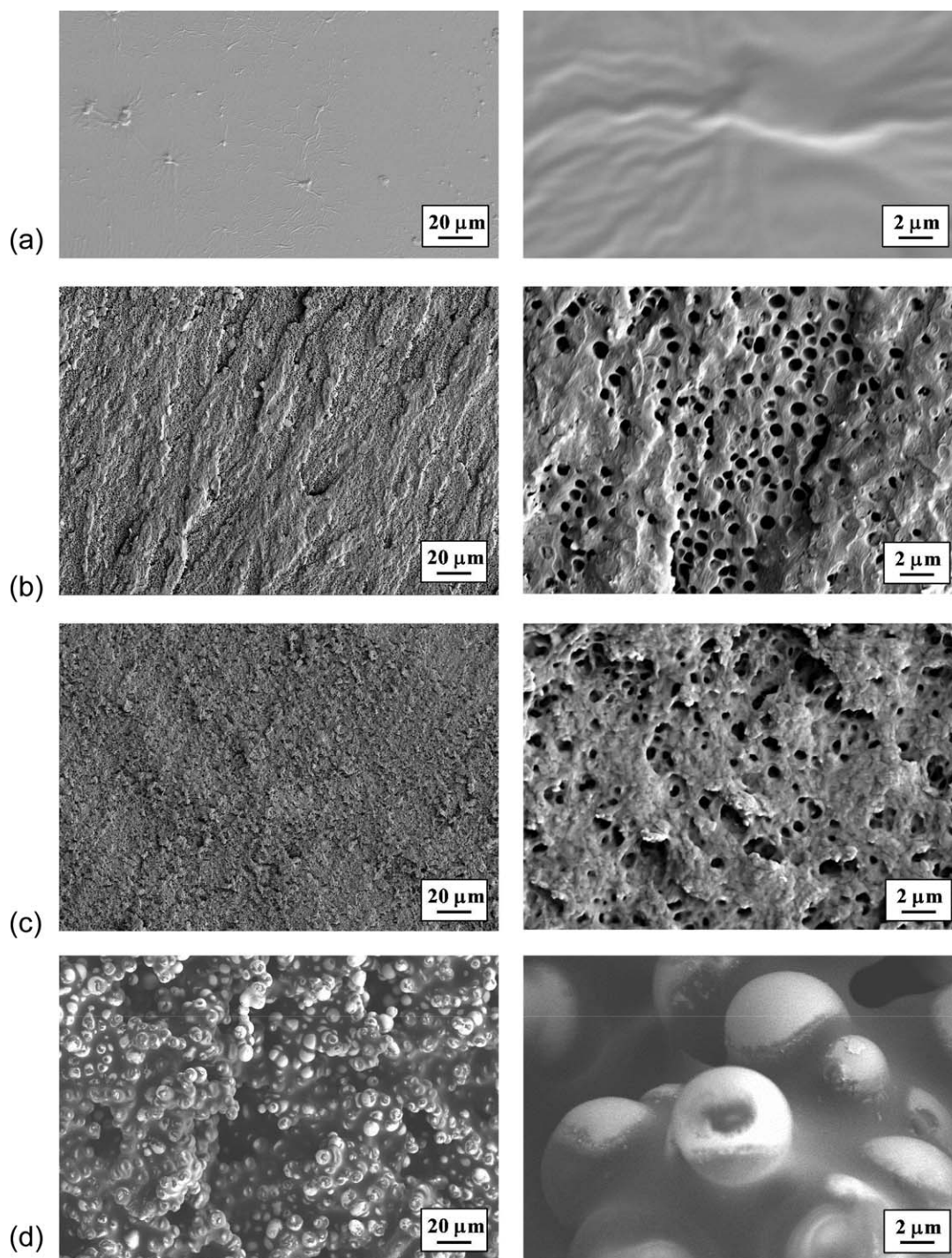


Figure 5. Micrographs of (a) System B, 26 vol % PEG, (b) System B, 44 vol % PEG, (c) System C, 65 vol % PEG, and (d) System B, 65 vol % PEG.

results show that phase separation alone is not sufficient to achieve good multifunctionality, but that the phases must be arranged properly and provide good individual functional performance. Further tuning of the processing and composition of System B could lead to a more suitable interpenetrating structure with a better multifunctional property balance. The use of a PEG electrolyte in System B places it at a further disadvantage, due to the lower conductivity of electrolytes that use PEG as a solvent as compared to those that use more polar solvents

such as PC. Selection of an appropriately compatible, highly conductive electrolyte could mitigate these concerns.²³

System C clearly exhibits the best multifunctional performance, and approaches our target region of the graph. This result demonstrates that using separate and dedicated porogens and electrolytes allows each material to be independently selected and optimized, so that an ideal percolated monolith structure can be combined with a highly conductive, best-performing electrolyte.

The superior performance of System C is consistent with a previous hypothesis that decoupling the structural phase from the conductive phase, and optimizing both the individual performance of each component as well as their integrated microstructure, would lead to improvements in multifunctional performance.¹⁹ System C provides further benefit to allowing for flexible selection of electrolyte to best address application needs, particularly chemical and thermal stability, without requiring specific interactions with the structural polymer such as swelling or phase separation. The open porosity could introduce problems with solvent evaporation that would need to be addressed either through device packaging or encasement, or through use of low vapor pressure solvents such as ionic liquids.

The primary shortcoming of System C is the relatively low mechanical properties relative to the baseline epoxy, most likely due to the partial PEG plasticization of the epoxy network. A fully biphasic system exhibiting no plasticization and good control over microstructure could be expected to invest the entirety of the liquid phase into generating interconnected pores to achieve optimized percolation of the liquid phase and measurable conductivity at much lower liquid concentrations. For a 50% voided epoxy the theoretical modulus of the material can be calculated using a variety of model approximations that depend, in part, on the microstructure, but a compressive modulus at or above 500 MPa would be consistent with many of these theories.¹⁹ Therefore, through improved processing, it should be possible to create a nonplasticized, highly networked epoxy porous monolith with up to four times higher modulus at similar conductivity to meet the current program goals. By tailoring the details of the three-dimensional monolith geometry and fill fraction, multifunctionality may be further optimized.

CONCLUSIONS

The results of this study show that, in order to achieve highly multifunctional structural electrolytes, an effective strategy is to create a material with distinct conductive and structural phases. Furthermore, it is necessary to both control the microstructure

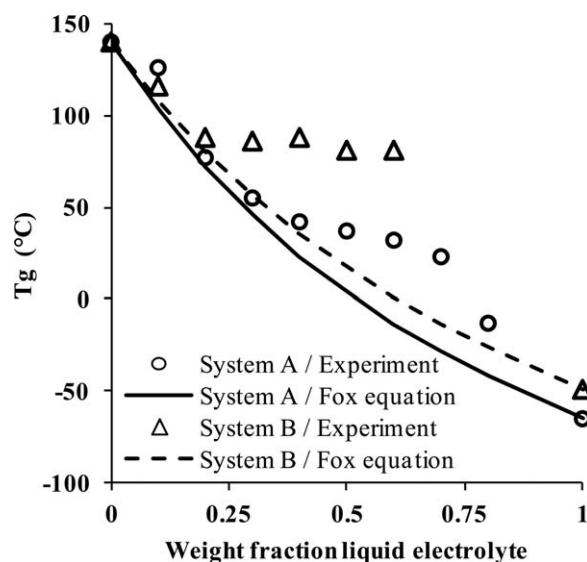


Figure 6. T_g as a function of liquid content in System A.

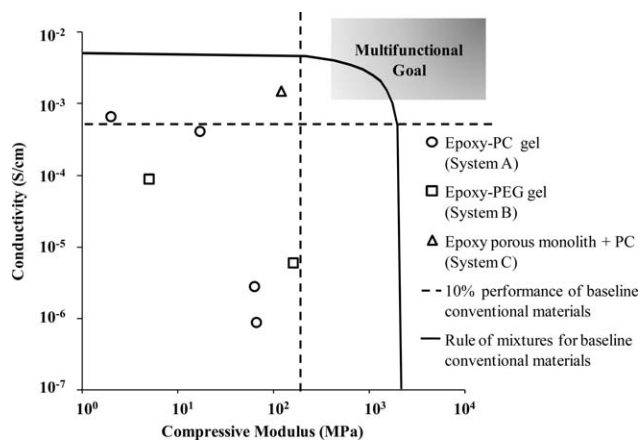


Figure 7. Multifunctional comparison of electrolyte material properties.

of the system, and ensure that the properties of each phase are optimized for their specific function. The approach of curing a structural polymer with liquid electrolyte *in situ* is attractive from a processing viewpoint, as it would be a convenient way to substitute a single-step structural electrolyte polymer for a conventional liquid electrolyte or structural polymer in a composite structural battery or supercapacitor system. However, this study shows that cocuring the structural and electrolyte polymers introduces a number of complications, and makes it difficult to control both microstructure and phase properties independently. Instead, selecting a polymer-porogen system to achieve an optimal microstructure, followed by exchange of the porogen for an optimal liquid electrolyte, is likely to be a more effective means of generating high performing multifunctional electrolytes.

A concern for additional study is the integration of these phase separating polymers with the separators, cathodes, and anodes that comprise a structural battery or supercapacitor. Phase separation can be greatly influenced by the presence of surfaces, so the microstructure in the vicinity of the electrode and separator surfaces may deviate from the idealized bulk morphologies shown in the present study.³² For example, preference for the epoxy phase by fiber surfaces can result in polymer “skins” that block access of electrolyte to the charge storage sites on the fiber. Further complication may be anticipated for processes such as demonstrated by System C in which the presence of fibers and complex interfaces may also inhibit removal of the porogen and subsequent introduction of electrolyte. Careful engineering of the material surfaces within the composite may be required to achieve desirable system-level performance. The approach demonstrated in System C should allow for a wide range of materials and processing steps to generate target interfaces.

ACKNOWLEDGMENTS

The authors gratefully acknowledge Hong Dong for help with microscopy. This research was supported in part by an appointment to the Postgraduate Research Participation Program at the U.S. Army Research Laboratory administered by the Oak Ridge

Institute for Science and Education through an interagency agreement between the U.S. Department of Energy and USARL.

REFERENCES

1. Gibson, R. F. *Compos. Struct.* **2010**, *92*, 2793.
2. Aglietti, G. S.; Schwingshackl, C. W.; Roberts, S. C. *Shock Vib. Digest* **2007**, *39*, 11.
3. Wetzel, E. D. *AMPTIAC Q.* **2004**, *8*, 91.
4. Thomas, J. P.; Qidwai, M. A. *Acta Mater.* **2004**, *52*, 2155.
5. Christodoulou, L.; Venables, J. D. *J. Miner. Metals Mater. Soc.* **2003**, *55*, 39.
6. Qian, H.; Kucernak, A. R.; Greenhalgh, E. S.; Bismarck, A.; Shaffer, M. S. P. *ACS Appl. Mater. Interfaces* **2013**, *5*, 6113.
7. Shirshova, N.; Qian, H.; Shaffer, M. S. P.; Steinke, J. H. G.; Greenhalgh, E. S.; Curtis, P. T.; Kucernak, A.; Bismarck, A. *Compos. A Appl. Sci. Manufact.* **2013**, *46*, 96.
8. Asp, L. E. *Plast. Rubber Compos.* **2013**, *42*, 144.
9. O'Brien, D. J.; Baechle, D. M.; Wetzel, E. D. *J. Compos. Mater.* **2011**, *45*, 2797.
10. Ekstedt, S.; Wysocki, M.; Asp, L. E. *Plast. Rubber Compos.* **2010**, *39*, 148.
11. Liu, P.; Sherman, E.; Jacobsen, A. *J. Power Sources* **2009**, *189*, 646.
12. Pereira, T.; Guo, Z. H.; Nieh, S.; Arias, J.; Hahn, H. T. *Compos. Sci. Technol.* **2008**, *68*, 1935.
13. Jacques, E.; Kjell, M. H.; Zenkert, D.; Lindbergh, G.; Behm, M. *Carbon* **2013**, *59*, 246.
14. Kim, H. C.; Sastry, A. M. *J. Intell. Mater. Syst. Struct.* **2012**, *23*, 1787.
15. Snyder, J. F.; Wong, E. L.; Hubbard, C. W. *J. Electrochem. Soc.* **2009**, *156*, A215.
16. Quartarone, E.; Mustarelli, P. *Chem. Soc. Rev.* **2011**, *40*, 2525.
17. Meyer, W. H. *Adv. Mater.* **1998**, *10*, 439.
18. Snyder, J. F.; Carter, R. H.; Wetzel, E. D. *Chem. Mater.* **2007**, *19*, 3793.
19. Snyder, J. F.; Wetzel, E. D.; Watson, C. M. *Polymer* **2009**, *50*, 4906.
20. Torquato, S.; Hyun, S.; Donev, A. *J. Appl. Phys.* **2003**, *94*, 5748.
21. Nguyen, P.-A. T.; Snyder, J. *ECS Trans.* **2008**, *11*, 73.
22. Shirshova, N.; Bismarck, A.; Greenhalgh, E. S.; Johansson, P.; Kalinka, G.; Marczewski, M. J.; Shaffer, M. S. P.; Wienrich, M. *J. Phys. Chem. C* **2014**, *118*, 28377.
23. Shirshova, N.; Johansson, P.; Marczewski, M. J.; Kot, E.; Ensling, D.; Bismarck, A.; Steinke, J. H. G. *J. Mater. Chem. A* **2013**, *1*, 9612.
24. Wang, J. L.; Du, Z. J.; Li, C. J.; Li, H. Q.; Zhang, C. *J. Appl. Polym. Sci.* **2009**, *111*, 746.
25. Wang, J. L.; Zhang, C.; Du, Z. J.; Xiang, A. M.; Li, H. Q. *J. Colloid Interface Sci.* **2008**, *325*, 453.
26. Hosoya, K.; Hira, N.; Yamamoto, K.; Nishimura, M.; Tanaka, N. *Anal. Chem.* **2006**, *78*, 5729.
27. ASTM Standard D695. Standard Test Method for Compressive Properties of Rigid Plastics; ASTM International: West Conshohocken, PA, **2010**.
28. Fox, T. G. *Bull. Am. Phys. Soc.* **1956**, *1*, 123.
29. Huang, Y. H.; Wang, J. Z.; Liao, B.; Chen, M. C.; Cong, G. M. *J. Appl. Polym. Sci.* **1997**, *64*, 2457.
30. Ue, M.; Mori, S. *J. Electrochem. Soc.* **1995**, *142*, 2577.
31. Fan, J.; Fedkiw, P. S. *J. Electrochem. Soc.* **1997**, *144*, 399.
32. Javaid, A.; Ho, K. K. C.; Bismarck, A.; Shaffer, M. S. P.; Steinke, J. H. G.; Greenhalgh, E. S. *J. Compos. Mater.* **2014**, *48*, 1409.